# CHAPTER 3 TEM SURVEY

## 3-1 Background and Objectives

The TEM (Transient Electro-Magnetic) survey, sensitive to conductive bodies, such as massive sulphide deposits, was conducted to clarify the nature of the sulphide mineralization within the area delineated by the results of the TDIP survey.

During the present survey, large fixed loops were located on the base of the anomalies extracted from the TDIP survey. Taking into consideration the remarkable response given by conductive materials, such as massive sulphide ores, this detailed method is useful to extract promising mineralization zones by estimating their locations and boundaries.

## 3-2 Survey Locations and Specifications

The geophysical TEM survey method was utilized in Ghuzayn, Zuha and Maqail areas by using large fixed loops. In relation to the amount work undertaken during the TEM survey, a total of 12 loops corresponding to 972 stations were carried out in this year, as indicated in Table II-3-1.

## 3-3 TEM Survey Method

### 3-3-1 Basic principles

The principle of the TEM system used in this survey is to energize an ungrounded loop situated on the surface of the earth, as illustrated in Fig.II-3-1. When the currents flowing in the loop are switched off, free electron conduction currents are induced (eddy currents) in the ground. The eddy currents are known to depend on the conductivity, size, and shape of the conductive body, and position with respect to the sensing loop. These eddy currents set up a secondary magnetic field, which can be detected by a receiver coil as a time-dependant decaying voltage (Fig.II-3-2). The measurement of the time dependent decaying voltage is a means of detecting conductors in the ground. This transient decay can be measured by a number of measurement channels recording the voltage at various delay times after the transmitted fields are switched off. According to Faraday's law, the quick shut-off of the primary magnetic field caused by the current termination induces a pulse of e.m.f. (voltage) in the surrounding media. The resulting eddy currents produced in nearby conductive material support a surrounding secondary magnetic field for the duration of the pulse. Thereafter, with no external e.m.f. to support it, this system of currents and magnetic field decays with time, and it is this transient magnetic field which the receiver measures. These measurements occur during fixed time "windows" which occupy most of the "off-time" of the transmitter. As the receiver must know when the transmitter is off, synchronization was done by using crystal clocks.

Table Ⅱ-3-1 Survey amounts of TEM

| AREA | Number of Loops | Number of Points |
|---|---|---|
| Ghuzayn | 2 | 162 |
| Zuha | 7 | 567 |
| Maqail | 3 | 243 |
| Total | 12 | 972 |

Table Ⅱ-3-2 Channel times after switch off

| Channel Number | Sampling Time ($\mu$ sec) | Window Width ($\mu$ sec) |
|---|---|---|
| 1 | 88 | 18 |
| 2 | 107 | 24 |
| 3 | 131 | 36 |
| 4 | 162 | 37 |
| 5 | 201 | 40 |
| 6 | 251 | 72 |
| 7 | 314 | 76 |
| 8 | 396 | 100 |
| 9 | 499 | 142 |
| 10 | 631 | 156 |
| 11 | 799 | 180 |
| 12 | 1014 | 250 |
| 13 | 1287 | 380 |
| 14 | 1636 | 390 |
| 15 | 2081 | 500 |
| 16 | 2648 | 720 |
| 17 | 3373 | 780 |
| 18 | 4297 | 1080 |
| 19 | 5475 | 1420 |
| 20 | 6978 | 1560 |

**3-3-2 Logistics and data acquisition**

There are several varieties of TEM systems and modes of operations. During this survey it was used the configuration of large fixed-loop. For the case of large loops, a large, single-turn square loop of wire of 600m by 600m is laid out on the ground. A portable power generator of 2500W fed a transmitter, which provides a series of alternating bipolar currents pulses with slow exponential turn-on and a rapid linear

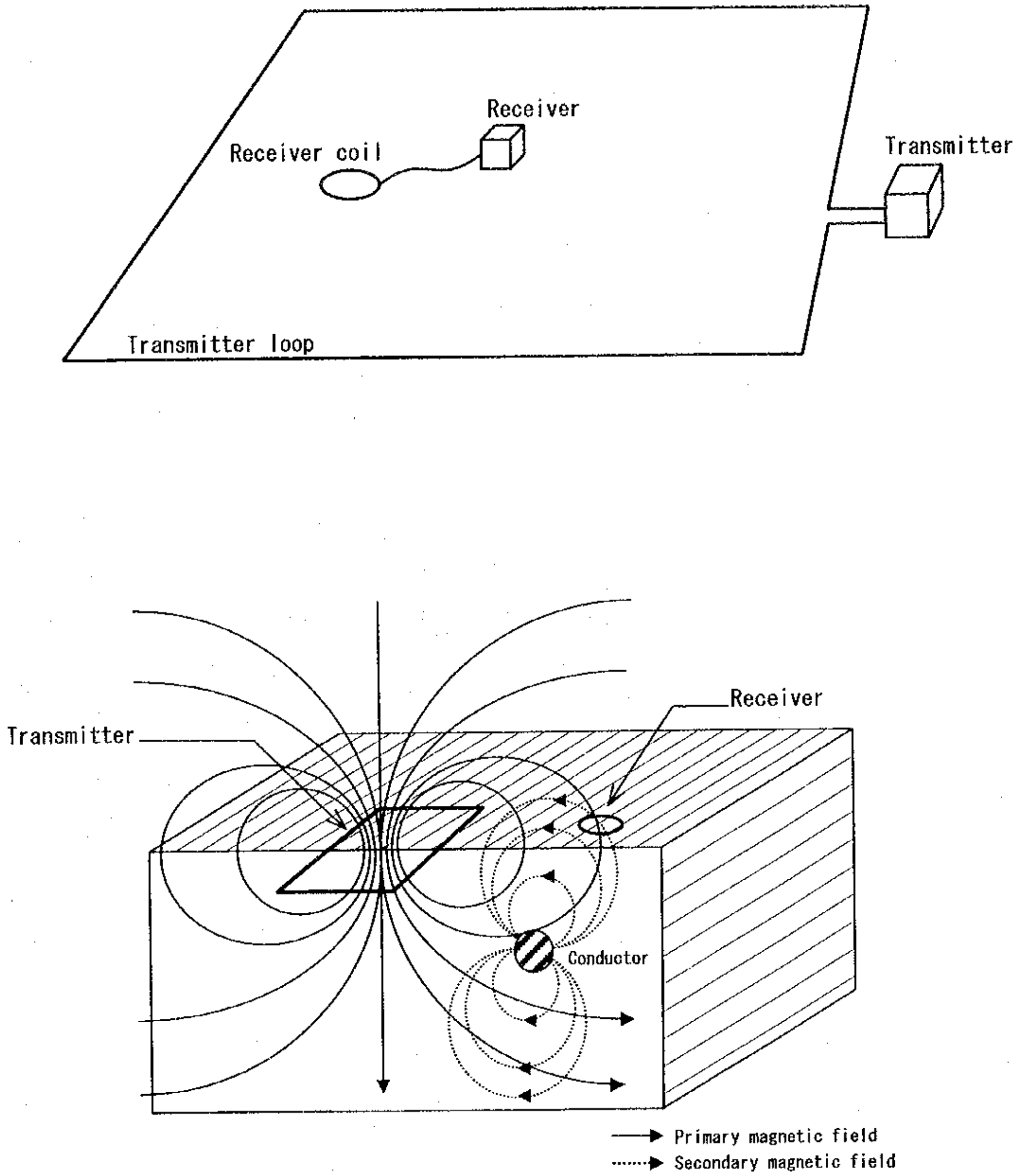


Fig. II -3-1 Schematic TEM survey configuration

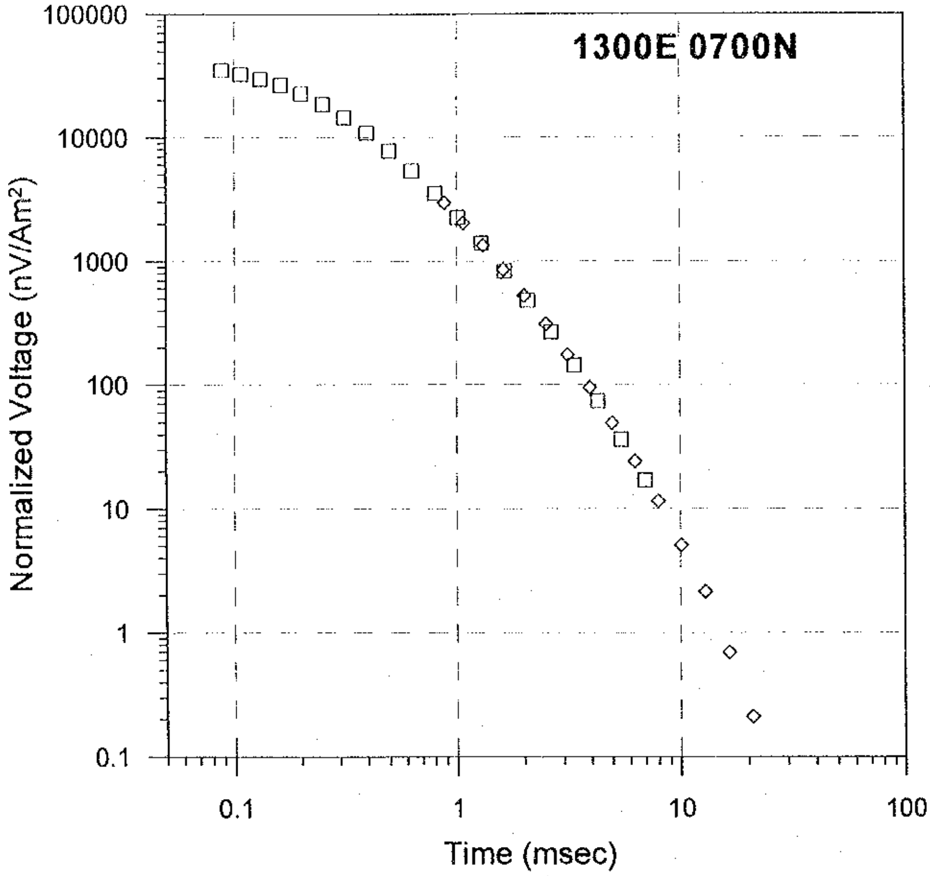


Fig. II-3-2 Example of TEM decay curve

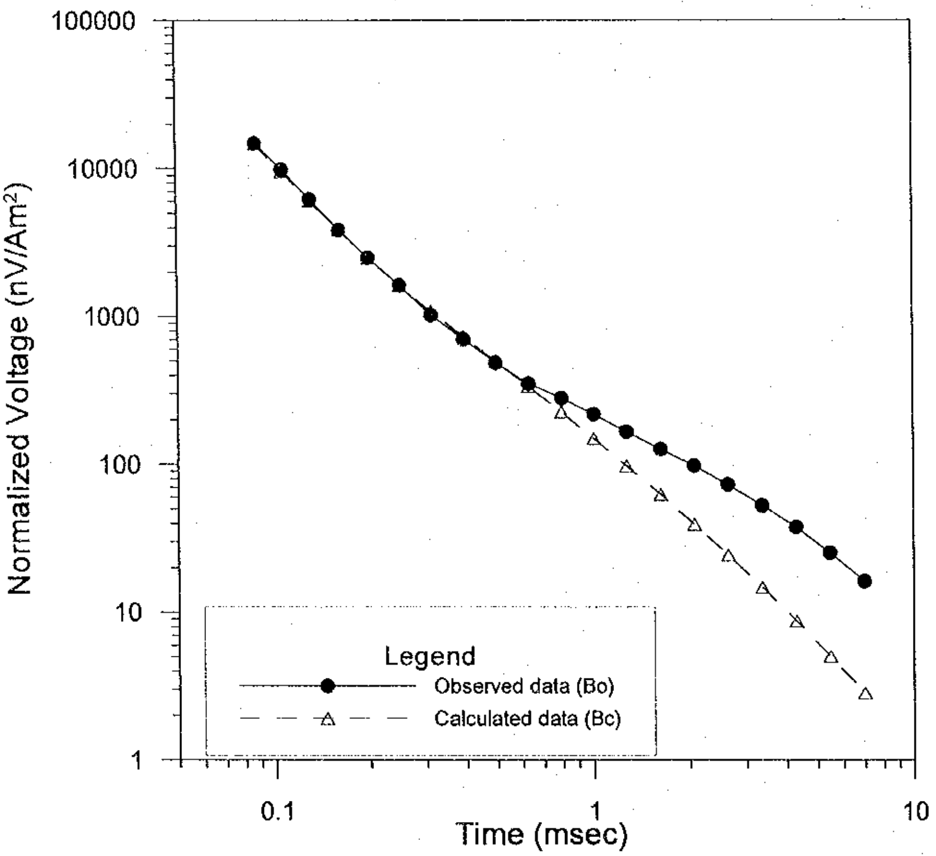


Fig. II-3-3 Observed and background TEM responses turn-off precise current waveform through the loop. After the transmitter loop has been set up, a small portable multi-coil receiver is moved to stations along surface lines inside the loop. Lines were surveyed within the loop to a distance of 100m away from the loop and the grid interval between the observed points was 50m.

Previous to the data acquisition, the crystals of the transmitter and receiver are warmed up before attempting to synchronize. Synchronization of the transmitter and receiver was carried out using the built-in high stability quartz crystal oscillators. Integration for each measurement was carried out over $2^8$ cycles.

The current waveform driven through the transmitter loop and the number of spacing of channels in the receiver are the main distinguishing features of this method. 20 time channels with locations and width are shown in Table II-3-2. Successive operations at 25Hz, then 2.5Hz, effectively gives 30 channels covering range from 88 $\mu$ sec. to 72 msec. A steady current is terminated rapidly by a 220 $\mu$ sec. ramp in large loops.

During data collection, several transient decays are recorded for each sounding. Readings are acquired at several receiver gains with opposite receiver polarities for each sounding location to eliminate any cultural noise. Many pulses of positive and negative polarities are stacked in a short period of time and averaged to remove any disturbance.

### 3-3-3 Equipment specifications

The EM37 system manufactured by Geonics Ltd. of Canada was utilized during the TEM survey of this year with the specifications as detailed in Table II-3-3. The receiver used is the Protem.

The current waveform in the transmitter consists of alternating bipolar current pulses with a slow exponential turn-on and a rapid linear turn-off. The base frequency of operation can be set at 2.5, 6.25 or 25 Hz, with corresponding window times of 71.9, 28.7, or 7.17 msec respectively. In this survey we used a base frequency of 25 Hz transmitter motor generator: 5 HP Honda gasoline engine coupled to 120 volt, 3 phase, 400Hz alternator.

At the receiver the induced voltage in the coil is measured in millivolts. Using the effective area of the coil and the gain of the receiver, these measurements are converted to the time derivative of the magnetic field in nanovolts/amp-meter$^2$.

Table II-3-3 Specifications of TEM survey instruments

| Items | Specification |
|---|---|
| Transmitter | Max output:30A,180V |
| Generator | 5HP,120V,3phase,400Hz |
| Receiver | 25Hz: 0.088-7.19ms |
| | 6.25Hz: 0.35-28.7ms |
| | 2.5Hz: 0.88-71.9ms |
| Magnetic Sensor | Induction Coil |
| | Effective area 100m$^2$ |
| Recorder | Protem,2Mb |

### 3-4 Analysis Method

The fact that the primary field is absents during measurement time, leads to "cleaner" data that is easier to interpret. The rate of decay of a conductor's magnetic field depends primarily on its size and conductance. Eddy currents decay rapidly in poor conductors, while those due to good conductors decay slowly, and the timing of the channels is such that only the effects of eddy currents due to the good conductors are seen in the later channels. In conductive environments, therefore, the response from overburden and weak mineralization should be minimal in the later channels where the target response predominates.

The first step in data processing is to average the e.m.f. (voltages) that are recorded at opposite receiver polarities. Then, the records at different amplifier gains are combined to give a single composite transient decay. After the composite transient decay has been calculated for each measurement point, the late stage apparent resistivities are calculated by using the following equation:

$$\rho_a(t) = \frac{\mu^{5/3} M_r^{2/3}}{20^{2/3}\pi} \cdot \frac{M_t^{2/3}}{t^{5/3} V^{2/3}}$$

Where $V$ is the voltage measured at the receiver, $Mr$ is the moment of the receiver, $Mt$ is the moment of the transmitter, $\mu$ is magnetic permeability, and $t$ is the time measured after transmitter switch off.

The TEM response detected in the receiver, depends not only on the electrical properties of the ground, but also on the location of receiving points and transmitter loop size, generally the highest response are observed at the center of the loop. To correct the response due to the receiving location, the following procedure was carried out:

From the TEM data obtained at the center of the transmitter loop, a layered resistivity structure was calculated by using an inversion analysis that assumes that this electrical structure represents an average resistivity in the loop.

By using the parameters of this resistivity structure, a synthetic response Bc(x, y) was calculated at all the points within the loop by taking also into account the relative position between the receiver and transmitter loop. If the resistivity structure at a point is nearly same as the average resistivity structure, the observed EM response should be almost the same as the calculated synthetic response, resulting in a minimal difference. On the contrary and if the average resistivity structure is not related to an anomaly but the point represents the location of the conductive body underlied, then the response becomes extremely high as compared with the synthetic response, and therefore, the difference between the responses becomes high, i.e.,

$$\Delta B(x,y) = \log(Bo(x,y) / Bc(x,y))$$

Where: B(x,y) is the difference of response, Bo(x,y) is the observed response, Bc(x,y) is the synthetic response, and log is the logarithm of base 10 (Fig.II-3-3).

Contour map of the difference in the TEM responses permit the clarification of anomalies (if any) by the contrast in the TEM response values.

For the depth estimation, the following formula is used:

$$d = \sqrt{500\rho\, t}$$

Where $\rho$ is the average resistivity( Ω -m), $t$ is the time(msec) and $d$ is the depth(meter)

## 3-5 Survey Results

Table II-3-4 indicates the estimated exploration depth based on the above mentioned formula. Since these values are calculated for a layered structure at the center of the loop, the calculated depth should be taken with caution because it does not always correspond to the real depth.

Table II-3-4 Depth estimation in survey area

| Channel | Ghuzayn | | Maqail | | | Zuha | | | | | | |
|---|---|---|---|---|---|---|---|---|---|---|---|---|
| | Loop-1 | Loop-2 | Loop-1 | Loop-2 | Loop-3 | Loop-1 | Loop-2 | Loop-3 | Loop-4 | Loop-5 | Loop-6 | Loop-7 |
| Ch-01 | 50 | 50 | 89 | 64 | 59 | 56 | 50 | 62 | 53 | 55 | 58 | 56 |
| Ch-02 | 55 | 56 | 99 | 72 | 65 | 63 | 56 | 69 | 59 | 61 | 65 | 62 |
| Ch-03 | 63 | 63 | 112 | 81 | 74 | 71 | 63 | 78 | 67 | 70 | 74 | 71 |
| Ch-04 | 70 | 71 | 126 | 92 | 83 | 80 | 71 | 88 | 75 | 78 | 83 | 79 |
| Ch-05 | 79 | 80 | 141 | 102 | 93 | 89 | 79 | 98 | 84 | 87 | 93 | 89 |
| Ch-06 | 89 | 90 | 159 | 115 | 105 | 100 | 89 | 110 | 95 | 99 | 105 | 100 |
| Ch-07 | 100 | 101 | 179 | 130 | 118 | 113 | 101 | 124 | 106 | 111 | 118 | 112 |
| Ch-08 | 112 | 113 | 200 | 145 | 132 | 126 | 112 | 138 | 119 | 124 | 131 | 126 |
| Ch-09 | 126 | 127 | 226 | 163 | 149 | 142 | 127 | 156 | 134 | 140 | 148 | 142 |
| Ch-10 | 141 | 143 | 253 | 183 | 167 | 159 | 142 | 175 | 150 | 157 | 166 | 159 |
| Ch-11 | 156 | 158 | 280 | 203 | 184 | 176 | 157 | 194 | 166 | 173 | 184 | 176 |
| Ch-12 | 174 | 176 | 312 | 226 | 205 | 196 | 175 | 216 | 185 | 193 | 205 | 196 |
| Ch-13 | 197 | 199 | 354 | 256 | 233 | 223 | 199 | 245 | 210 | 219 | 232 | 222 |
| Ch-14 | 222 | 225 | 399 | 289 | 262 | 251 | 224 | 276 | 237 | 247 | 262 | 250 |
| Ch-15 | 248 | 251 | 445 | 322 | 293 | 280 | 250 | 308 | 265 | 276 | 292 | 280 |
| Ch-16 | 280 | 284 | 503 | 364 | 331 | 317 | 282 | 348 | 299 | 311 | 330 | 316 |
| Ch-17 | 315 | 319 | 566 | 409 | 372 | 356 | 317 | 391 | 336 | 350 | 371 | 355 |
| Ch-18 | 352 | 356 | 632 | 457 | 416 | 398 | 355 | 437 | 375 | 391 | 415 | 397 |
| Ch-19 | 397 | 402 | 713 | 516 | 469 | 449 | 400 | 493 | 423 | 441 | 468 | 448 |
| Ch-20 | 447 | 452 | 801 | 580 | 527 | 505 | 450 | 555 | 476 | 496 | 526 | 503 |

### 3-5-1 Ghuzayn area

**(1) Loop locations**

A TEM survey by using 2 large loops was carried out based on high chargeability anomalies detected from the TDIP survey carried out on previous years in Ghuzayn. As in previous years, the data acquisition followed the description given in section 3-3-2 of this chapter. The TEM data were taken within a square loop of 400m by 400m with center in the center of the transmitter loop. Fig.II-2-4 illustrates the locations of the 2 large loops within Ghuzayn area.

**(2) Results**

Loop 1

Figs.II-3-4(1) and II-3-4(2) show the TEM responses obtained from the Loop1 at different channels, i.e. from channel 1 to channel 20.

High TEM responses were detected in the central part of the loop from channels 1 to 8 indicating the shallow response of the anomaly. Drilling survey was carried out on the center of this anomaly (MJOB-G43). Fig.II-3-6 shows the TEM response profile including the location of the borehole MJOB-G43.

Loop 2

Figs.II-3-5(1) and II-3-5(2) show the TEM results obtained within this loop.

High TEM responses were detected in the lower right part of this loop from the channels 1 to 15. This anomaly is found from shallow depth and showing a tendency to extend along a NW direction. It is very likely that this anomaly is associated to a fault, however, these results should be taken with caution because the results were somewhat affected by a power line close to the loop.

**3-5-2 Zuha area**

**(1) Loops locations**

The TEM survey was designed on the basis of the IP anomalies detected during the TDIP survey carried during this year. The TEM survey consisted of 7 large fixed loops with their locations indicated in Fig.II-2-20

**(2) Results**

Loop 1

Figs.II-3-7(1) and II-3-7(2) show the contour maps of the TEM responses obtained in each of the 20 channels.

High TEM response is seen in the left lower part of the loop and observed especially in the channels from 5 to 15 with decreasing values as it moves to the upper right side. These results are in agreement with the results obtained from the TDIP survey, which detected low resistivity with low chargeability values in this zone. Therefore, this low resistivity value does not appear to be related with mineralization related to massive sulphide.

Loop 2

Figs.II-3-8(1) and II-3-8(2) show the contour maps of the TEM responses obtained in each of the 20 channels. The TEM responses are seen rather weak with no remarkable anomaly for which it can be inferred that there exists a very low possibility of detecting massive sulphide ore body within this loop.

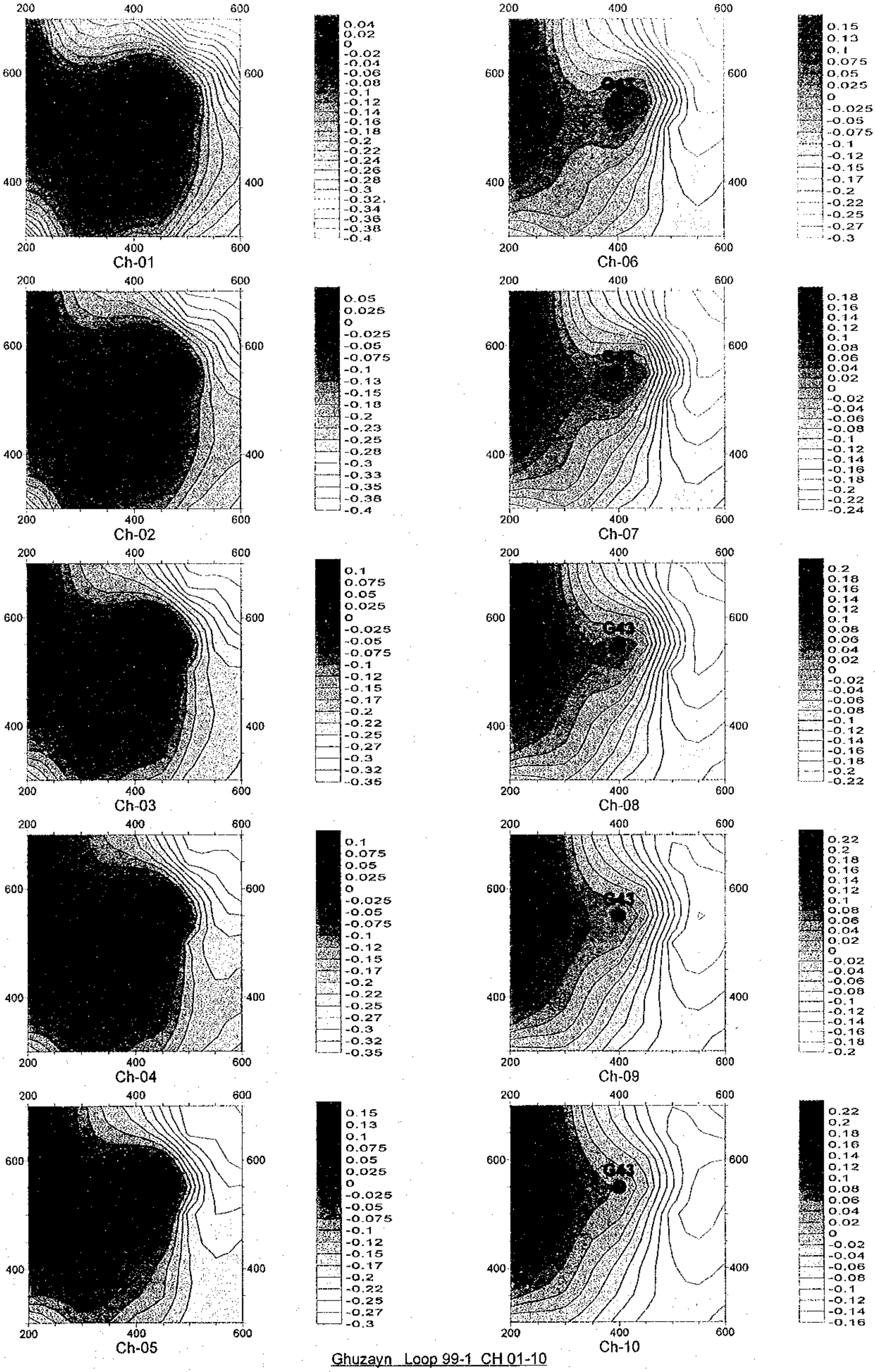


Fig. II-3-4(1) TEM response maps of Loop1 in Ghuzayn area(Ch1-Ch10)

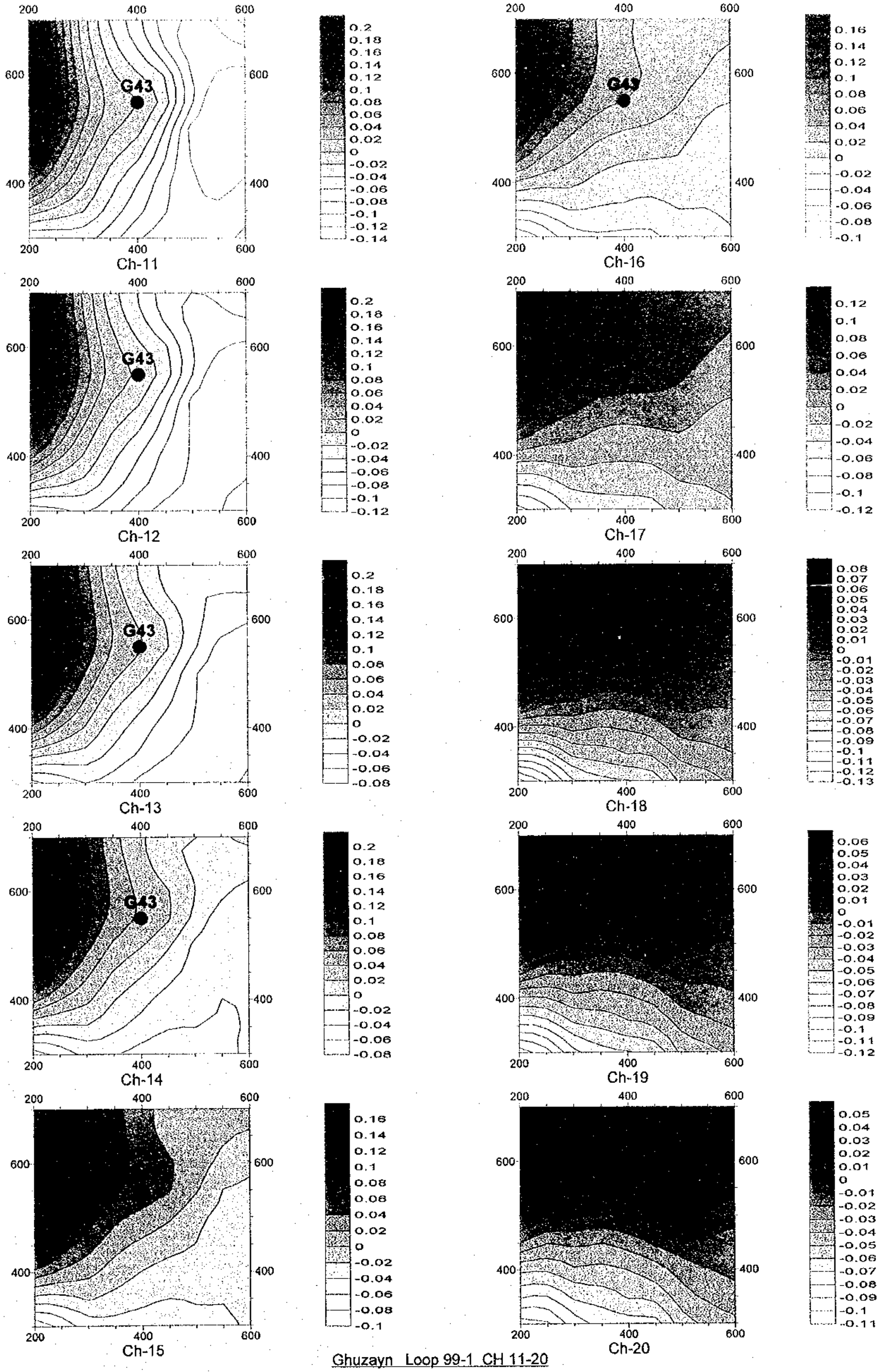


Fig. II -3-4(2) TEM response maps of Loop1 in Ghuzayn area(Ch11-Ch20)

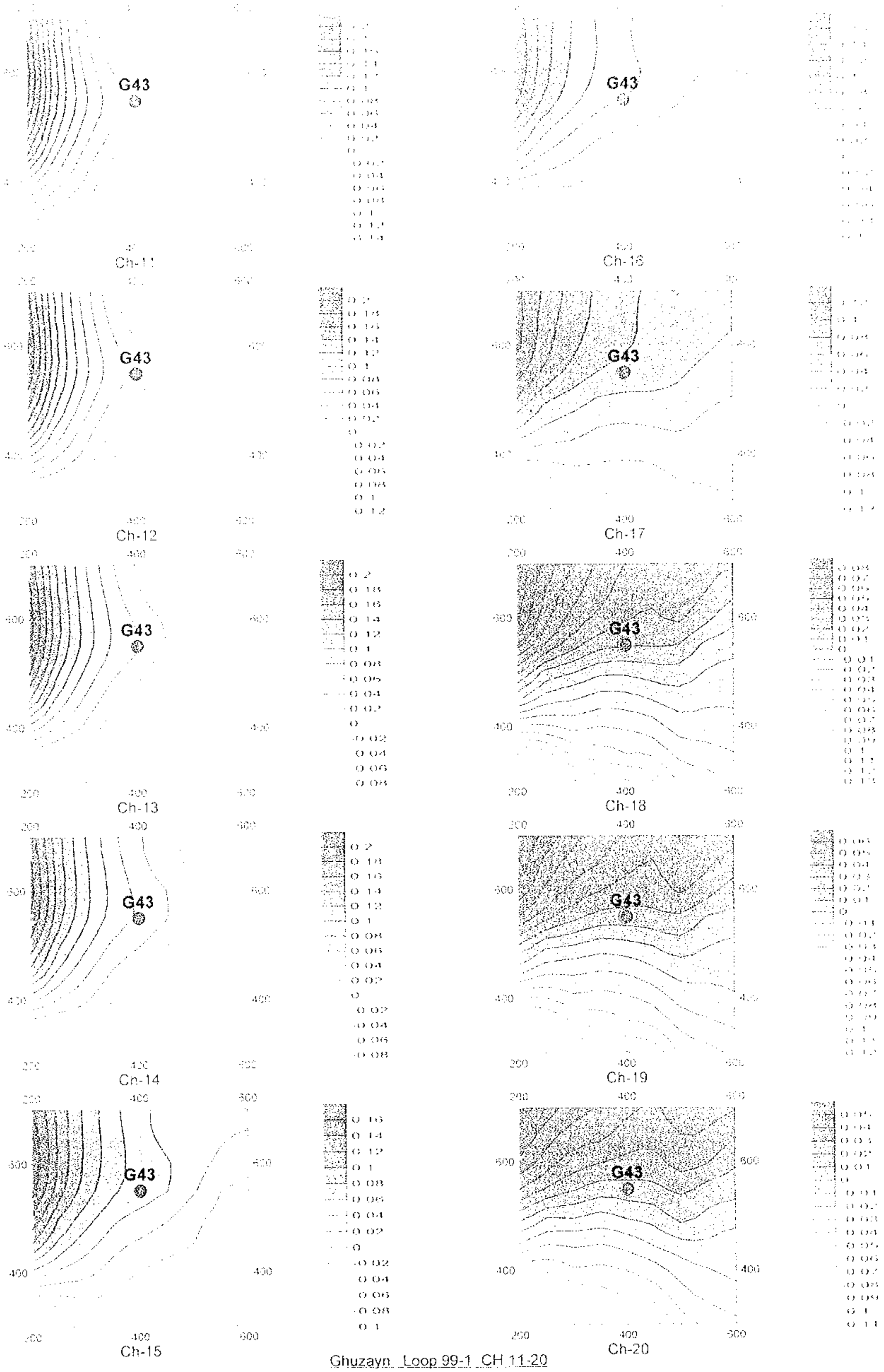


Fig. II-3-4(2) TEM response maps of Loop1 in Ghuzayn area(Ch11-Ch20)

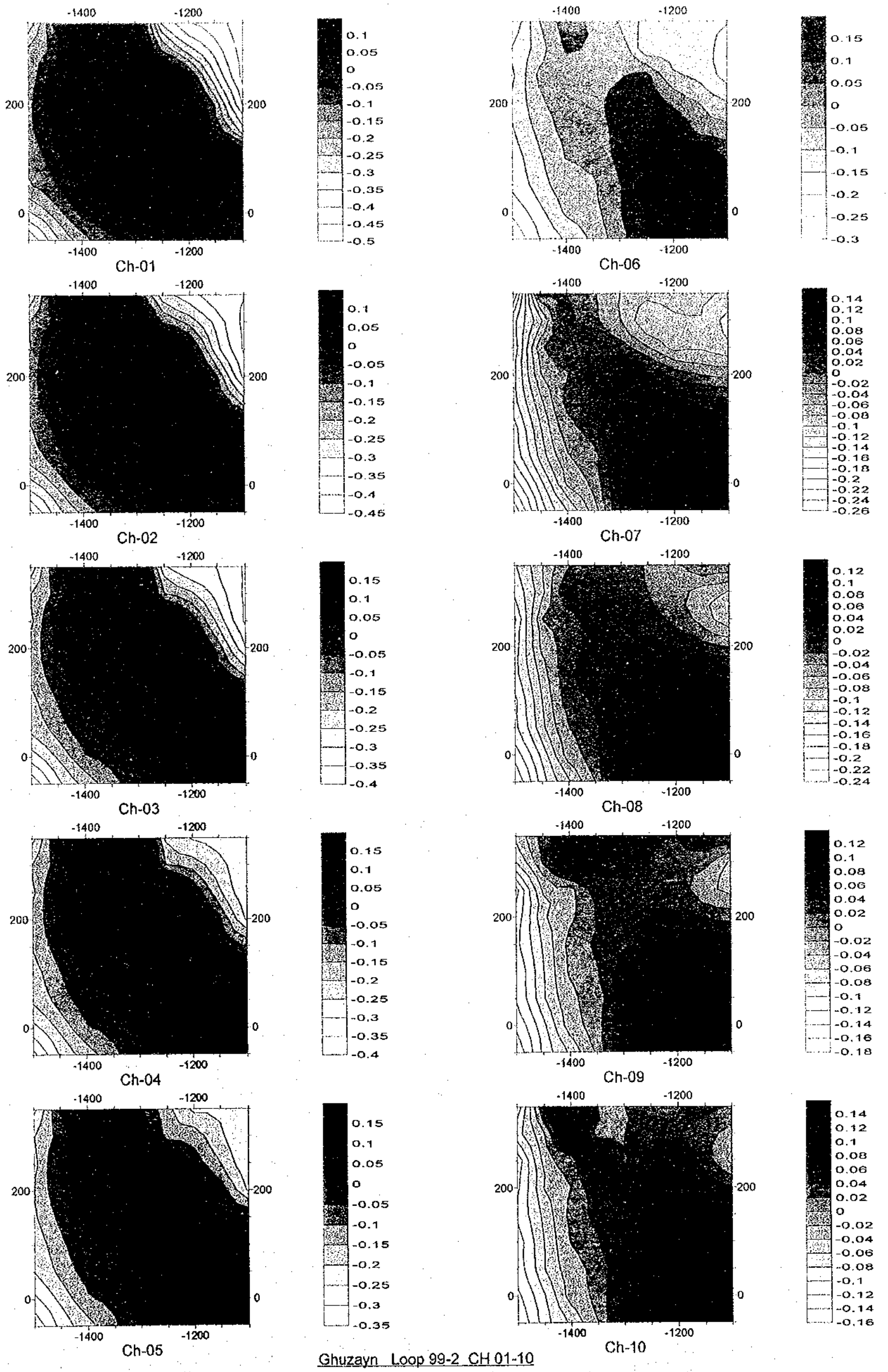


Fig. II -3-5(1) TEM response maps of Loop2 in Ghuzayn area(Ch1-Ch10)

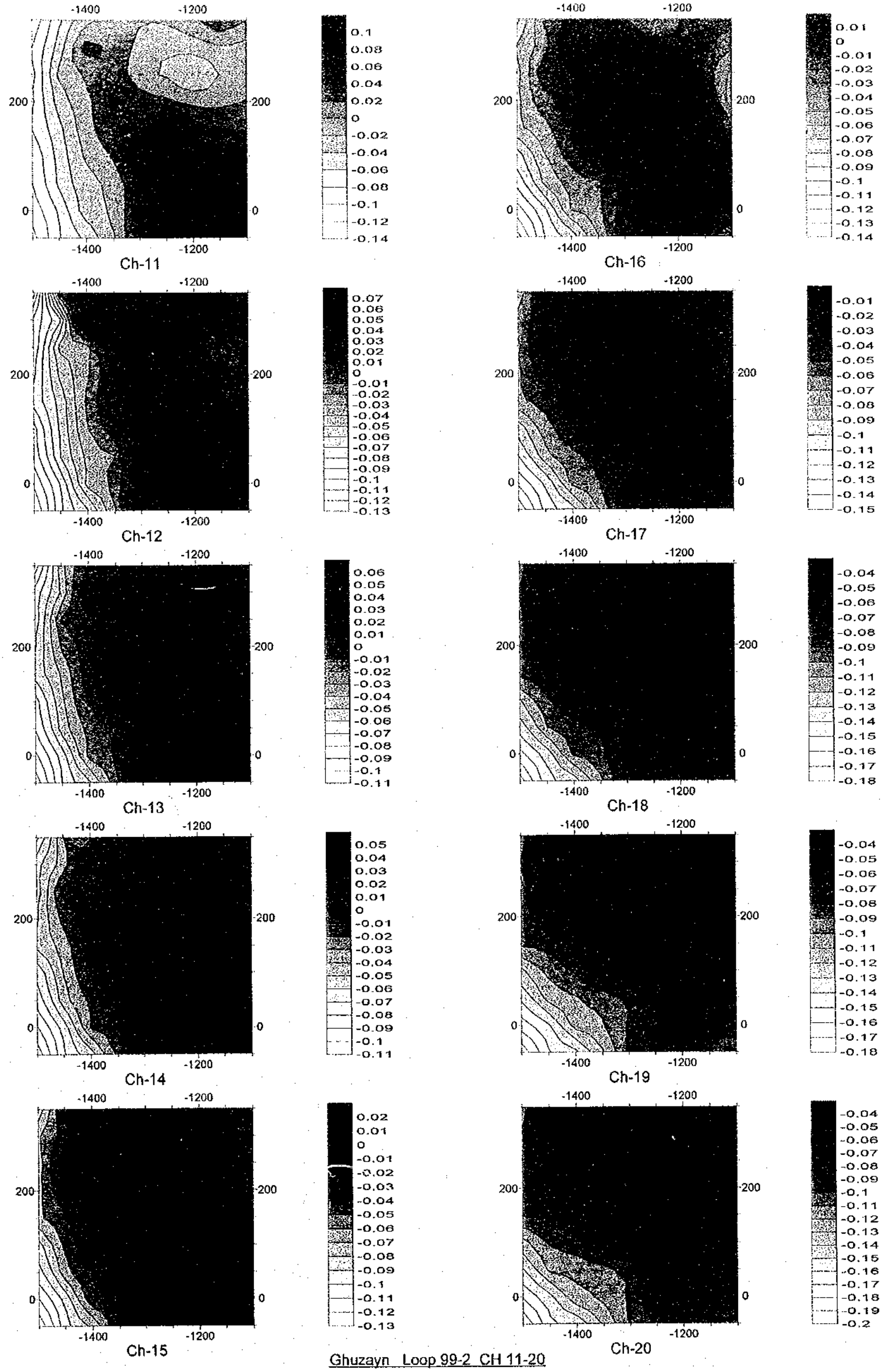


Fig. II-3-5(2) TEM response maps of Loop2 in Ghuzayn area(Ch11-Ch20)

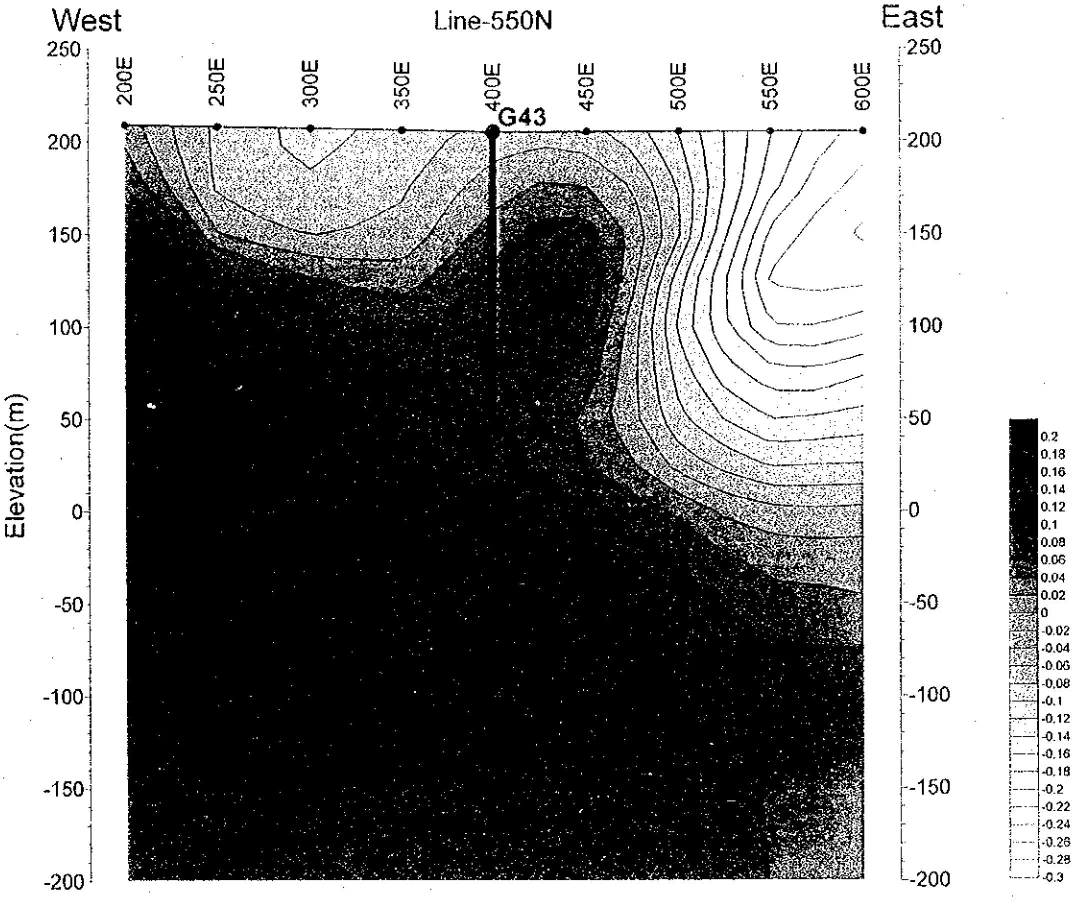


Fig. II -3-6 TEM response profile crossing drilling holes in Ghuzayn area

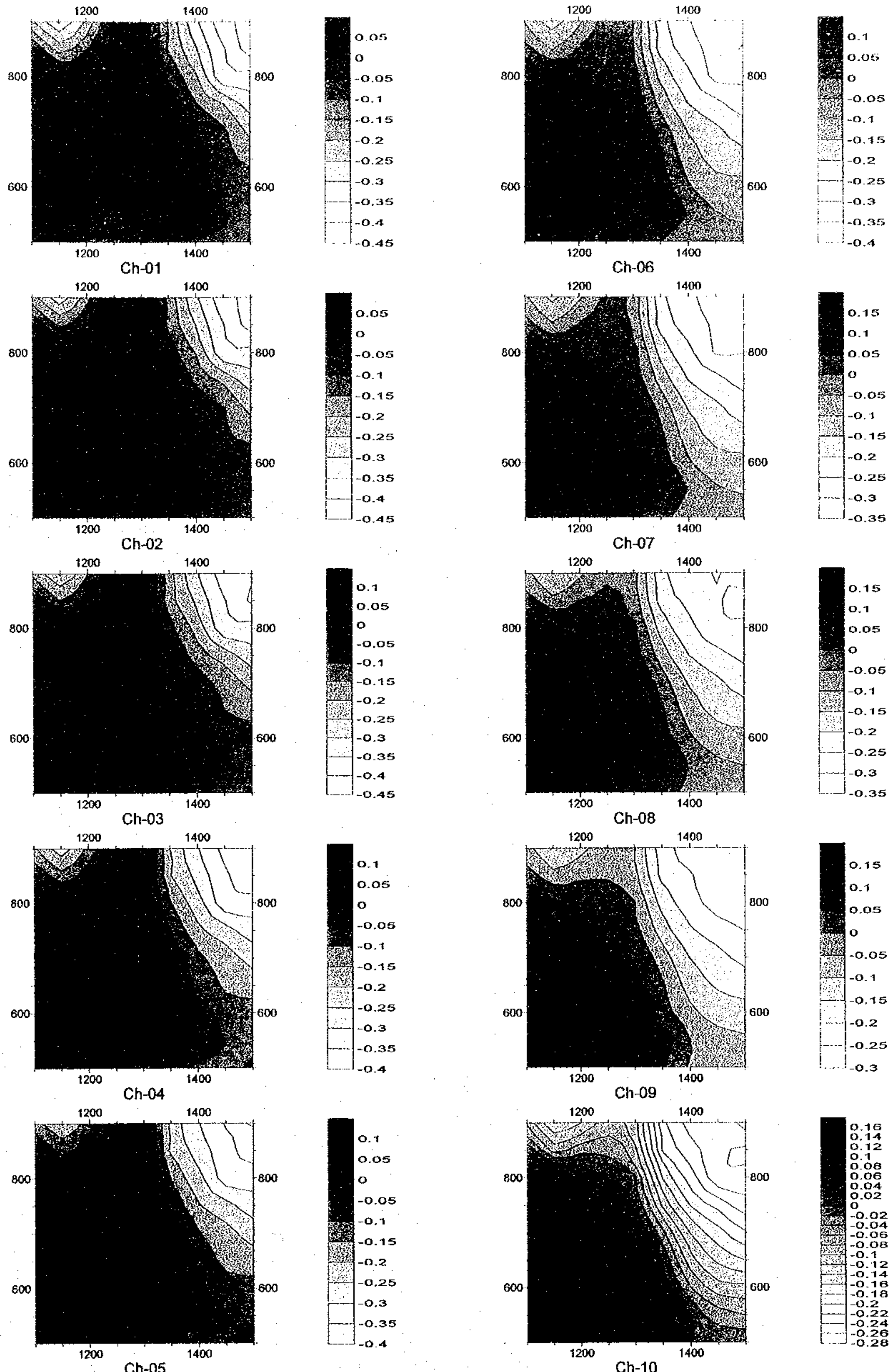


Zuha Loop 99-1 CH 01-10

Fig. Ⅱ-3-7(1) TEM response maps of Loop1 in Zuha area(Ch1-Ch10)

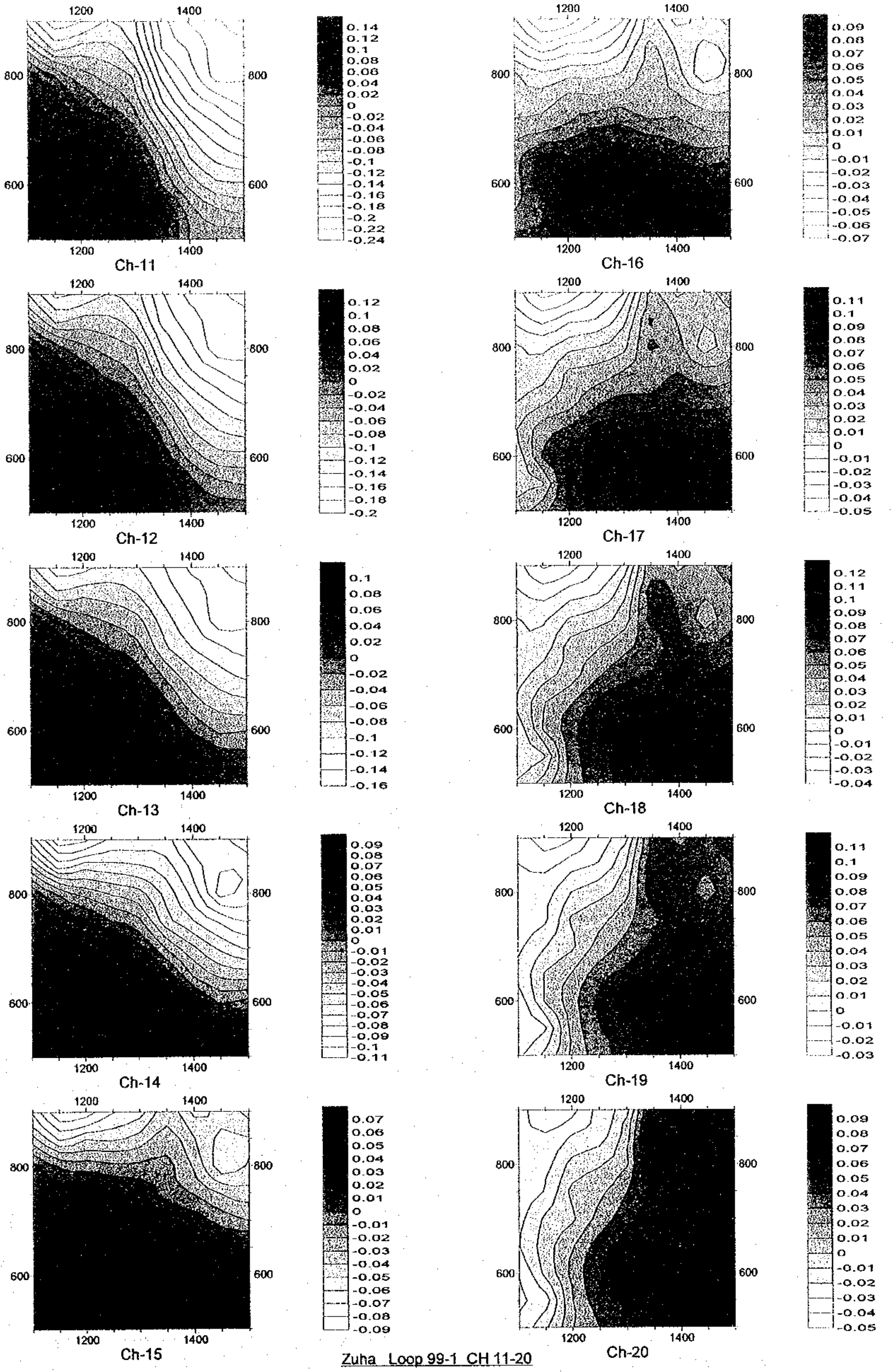


Fig. II-3-7(2) TEM response maps of Loop1 in Zuha area(Ch11-Ch20)

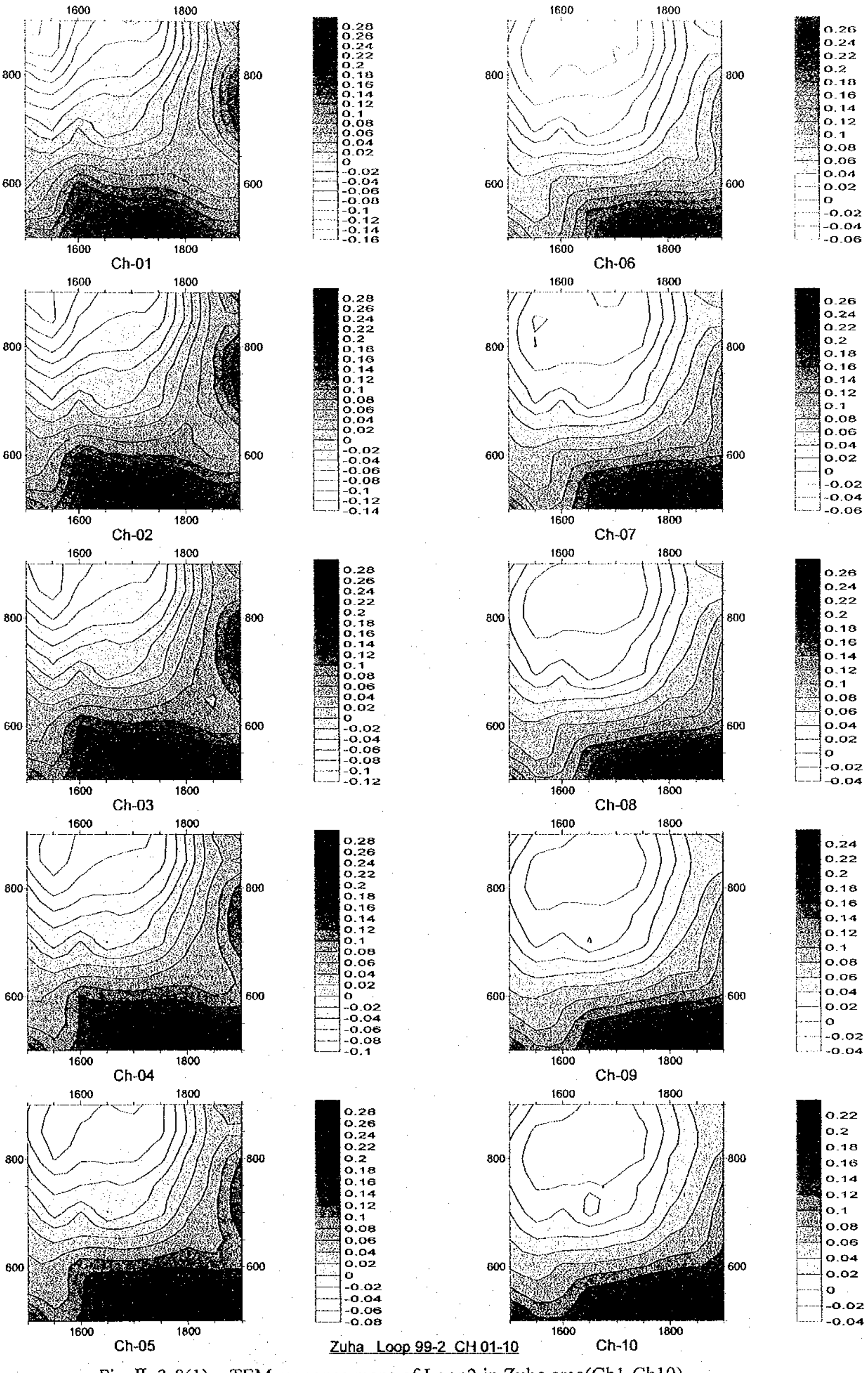


Fig. II-3-8(1) TEM response maps of Loop2 in Zuha area(Ch1-Ch10)

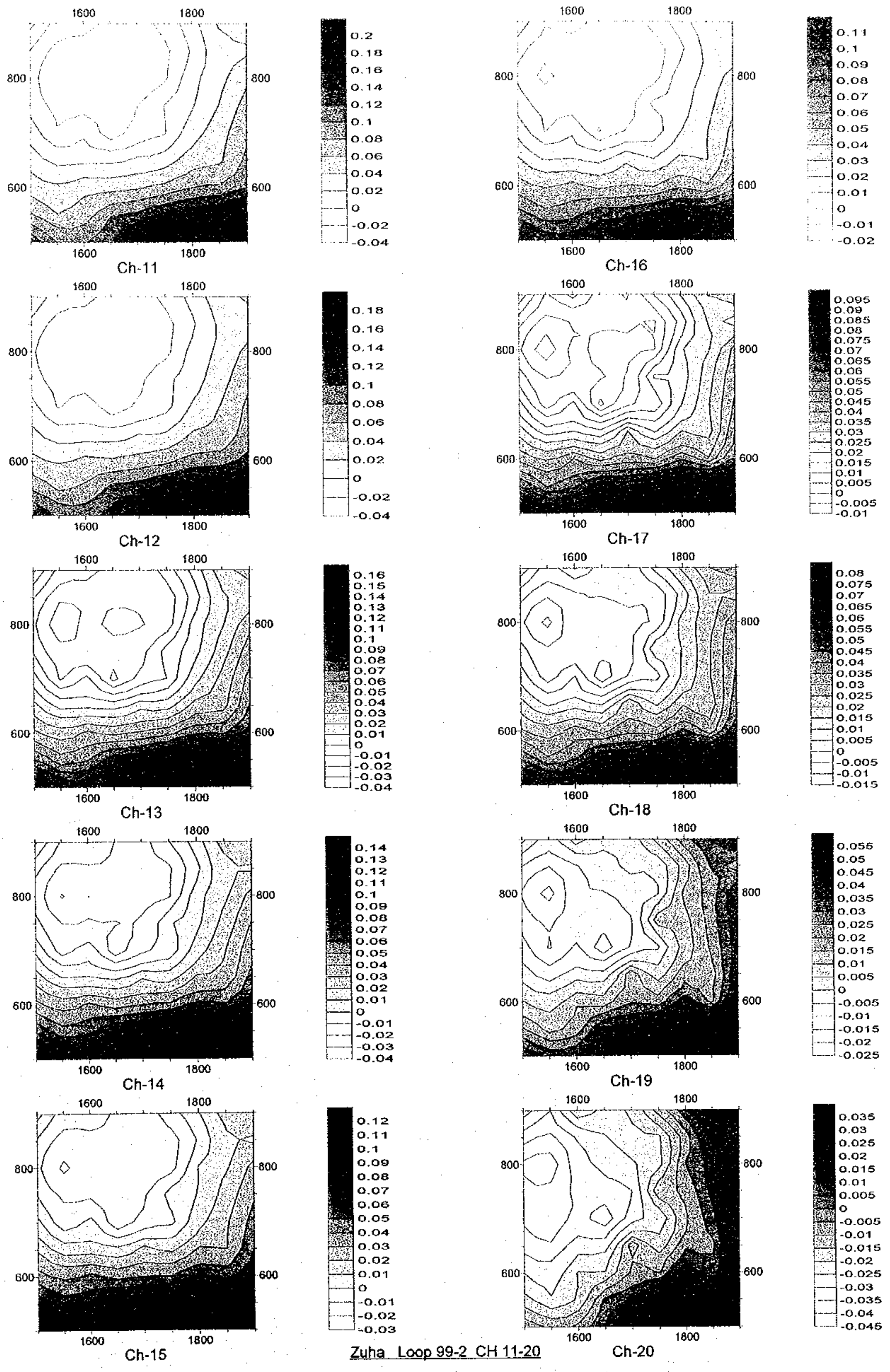


Fig. II -3-8(2) TEM response maps of Loop2 in Zuha area(Ch11-Ch20)

Loop3

Figs.II-3-9(1) and II-3-9(2) show the contour maps of the TEM responses obtained in each of the 20 channels. Comparatively high TEM responses are seen from the channels 5 to 12 in the central left part of the loop and with a tendency to decrease gradually towards the upper right side of the loop. No indications for the existence of any massive sulphide deposit are seen in this loop.

Loop4

Figs.II-3-10(1) and II-3-10(2) show the contour maps of the TEM responses obtained in each of the 20 channels. High TEM responses are seen in the right side of this loop through all the channels with a tendency to decrease gradually toward the left side of the loop. No indications for the existence of any massive sulphide deposit are seen in this loop.

Fig. II-3-14 shows the TEM response profile including the location of the borehole MJOB-Z1.

Loop5

Figs.II-3-11(1) and II-3-11(2) show the contour maps of the TEM responses obtained in each of the 20 channels. The results of the loop5 show a TEM response pattern similar to the results of loop4, for which it can be inferred that there is no indications for the existence of any massive sulphide within this loop.

Loop6

Figs.II-3-12(1) and II-3-12(2) show the contour maps of the TEM responses obtained in each of the 20 channels. The results of the loop5 show a TEM response pattern similar to the results of the previous 2 loops, for which it can be inferred that there are no indications for the existence of any massive sulphide within this loop.

Loop7

Figs.II-3-13(1) and II-3-13(2) show the contour maps of the TEM responses obtained in each of the 20 channels.

High TEM response is seen in the channels from 1 to 11 in the lower left side of the loop. These results seem to be an extension of the results obtained in loop 6.

### 3-5-3 Maqail area

#### (1) Loop locations

In Maqail, the TEM survey was designed on the basis of the IP anomalies detected during the TDIP survey carried during these last 2 years.

In this area and since relatively high chargeabilities were widely distributed in the west, central an north parts of the survey area, the TEM survey was set up in places which also meet the requirement of relatively low resistivity and high metal factor. In Maqail area, The TEM survey consisted of 3 large fixed loops with their locations indicated in Fig.II-2-29.

#### (2) Results

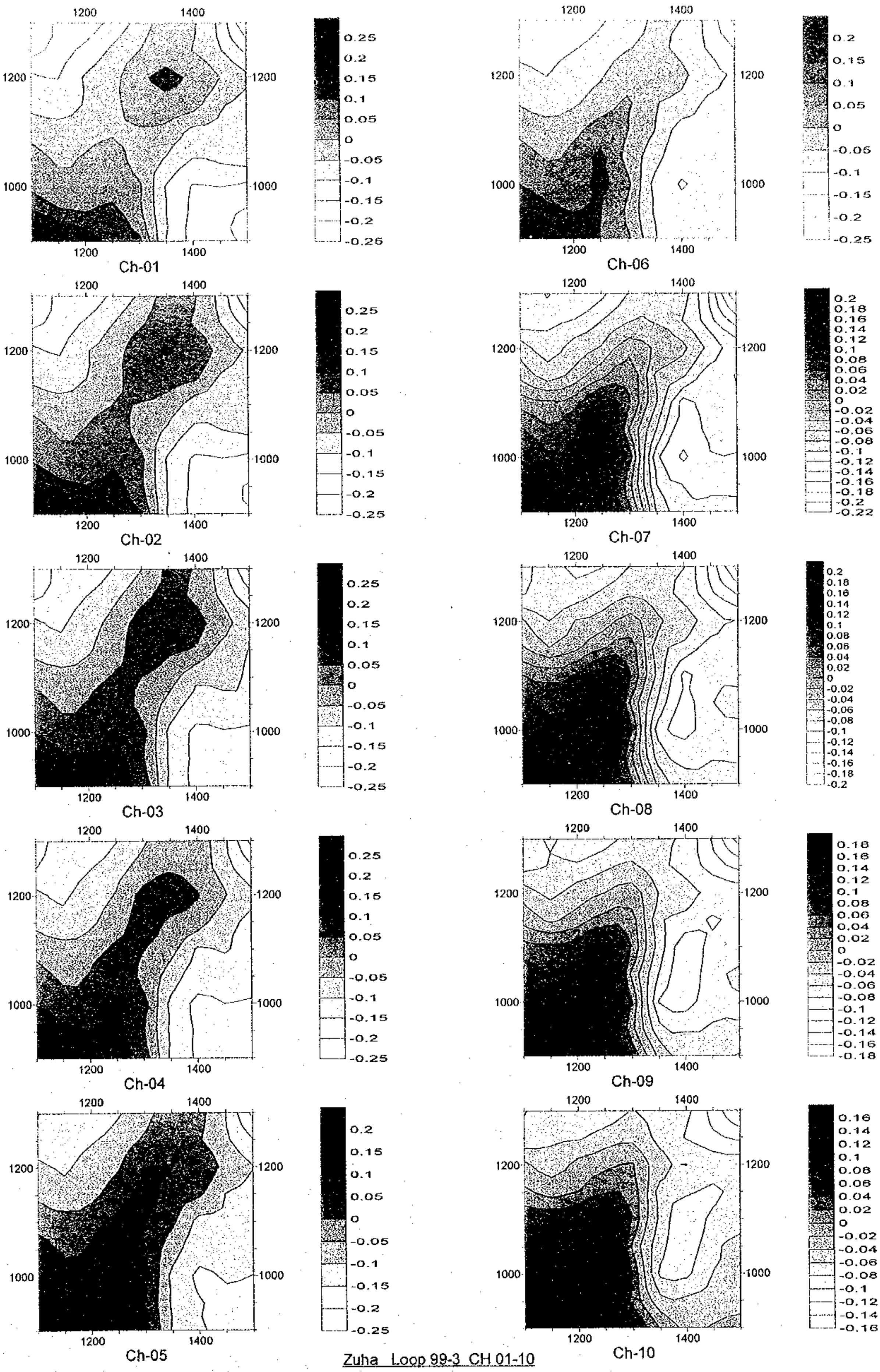


Fig. II -3-9(1) TEM response maps of Loop3 in Zuha area(Ch1-Ch10)

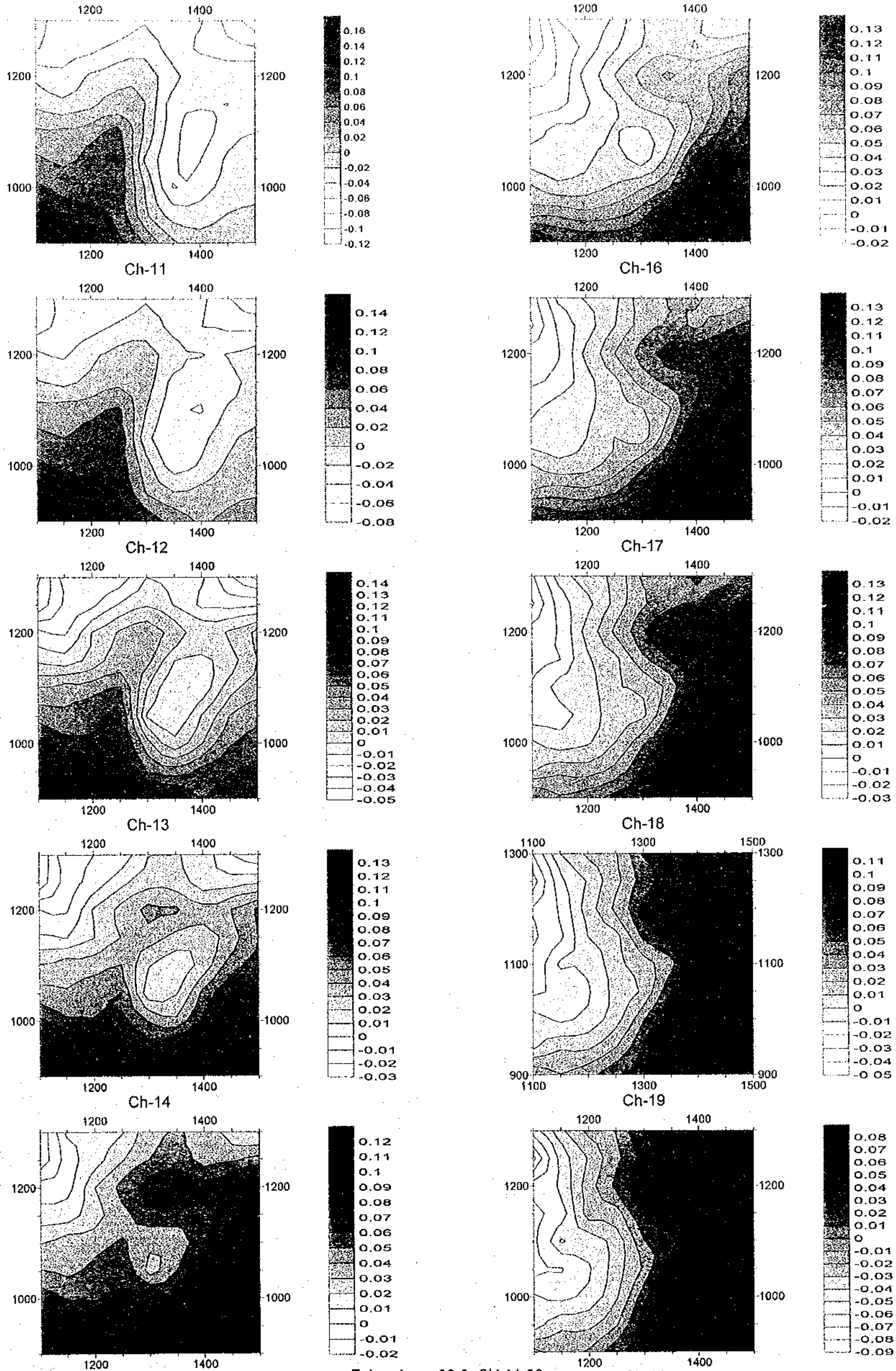


Fig. II-3-9(2) TEM response maps of Loop3 in Zuha area(Ch11-Ch20)

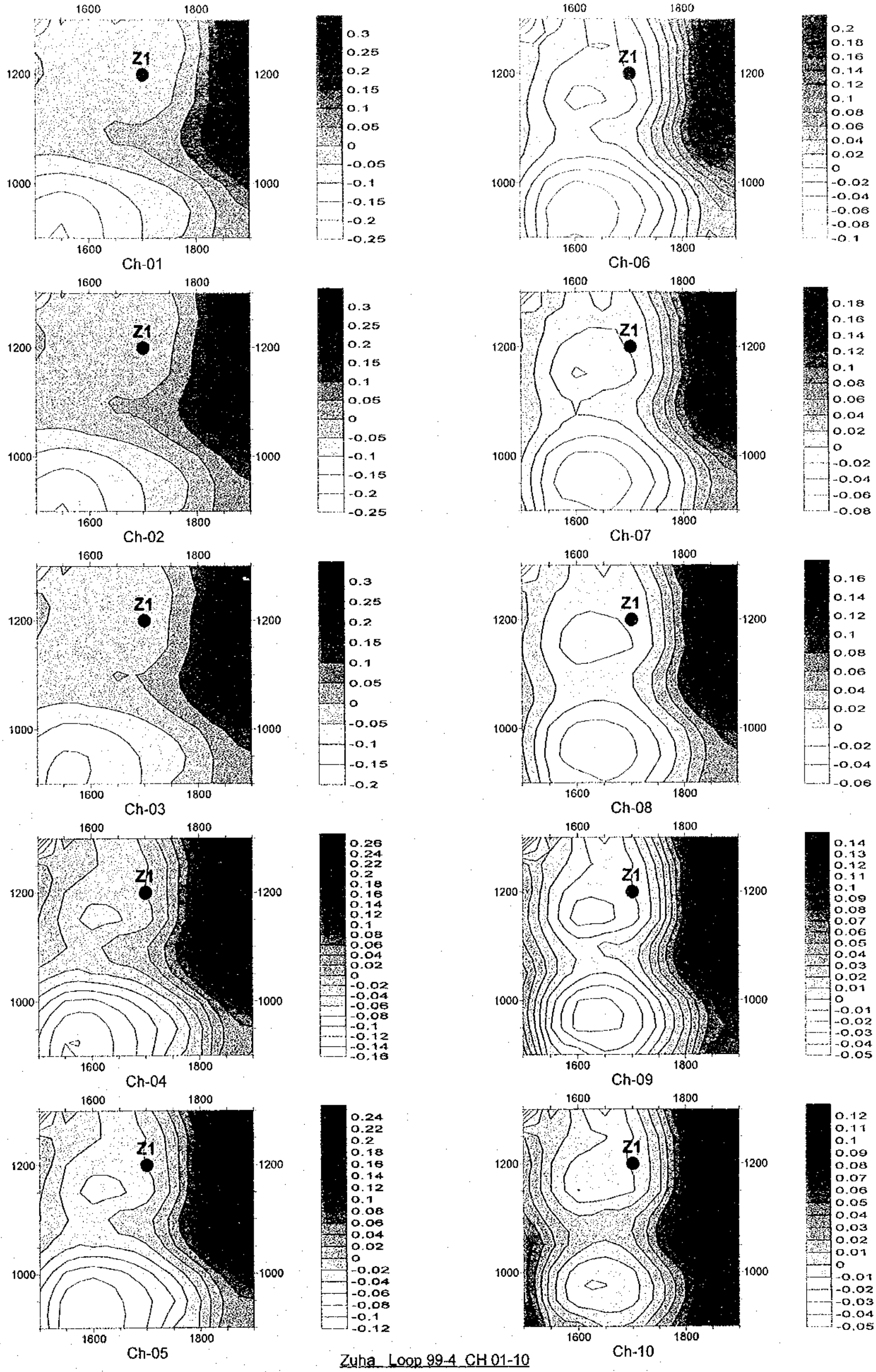


Fig. II-3-10(1) TEM response maps of Loop4 in Zuha area(Ch1-Ch10)

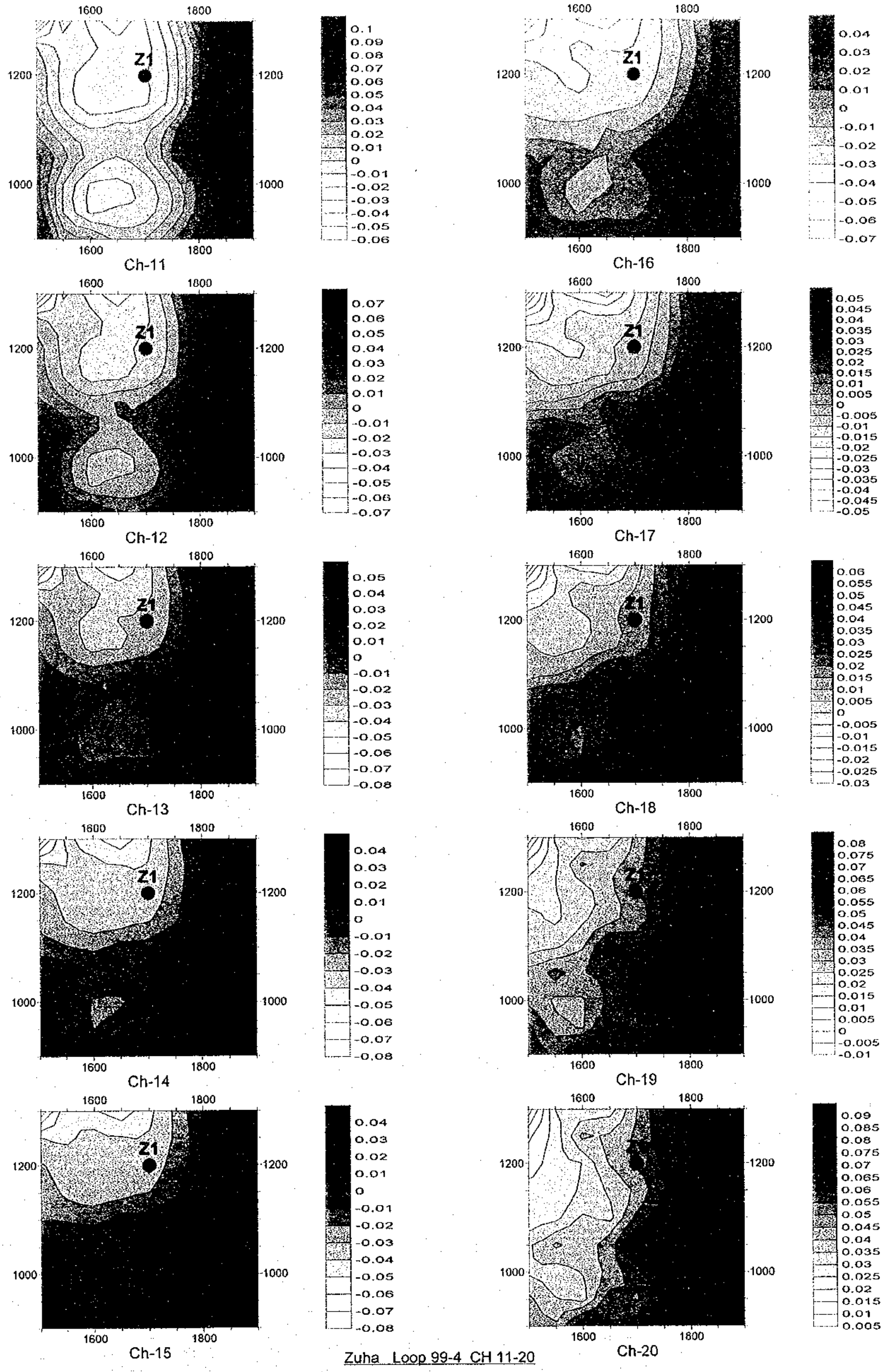


Fig. II-3-10(2) TEM response maps of Loop4 in Zuha area(Ch11-Ch20)

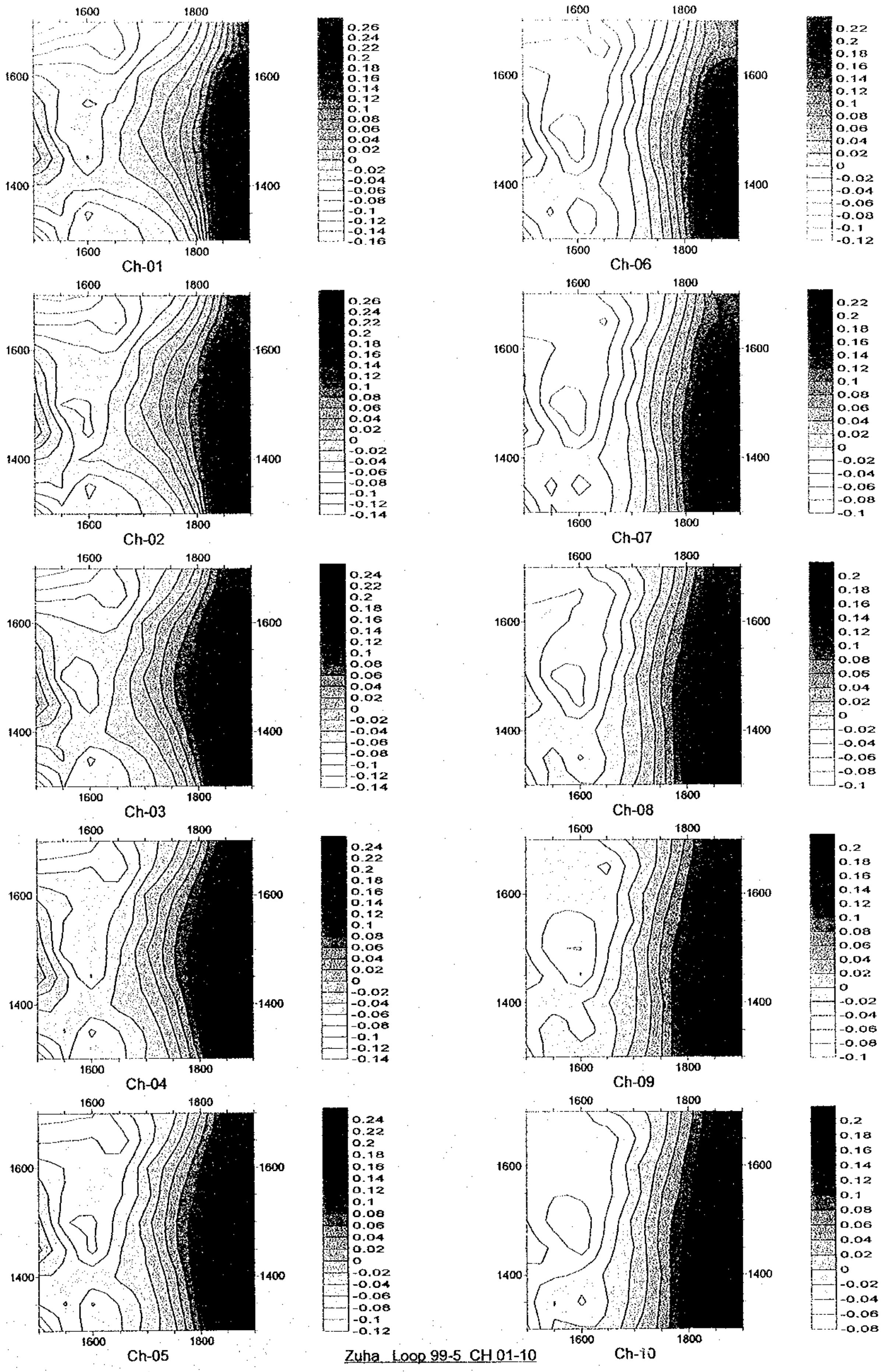


Fig. II-3-11(1) TEM response maps of Loop5 in Zuha area(Ch1-Ch10)

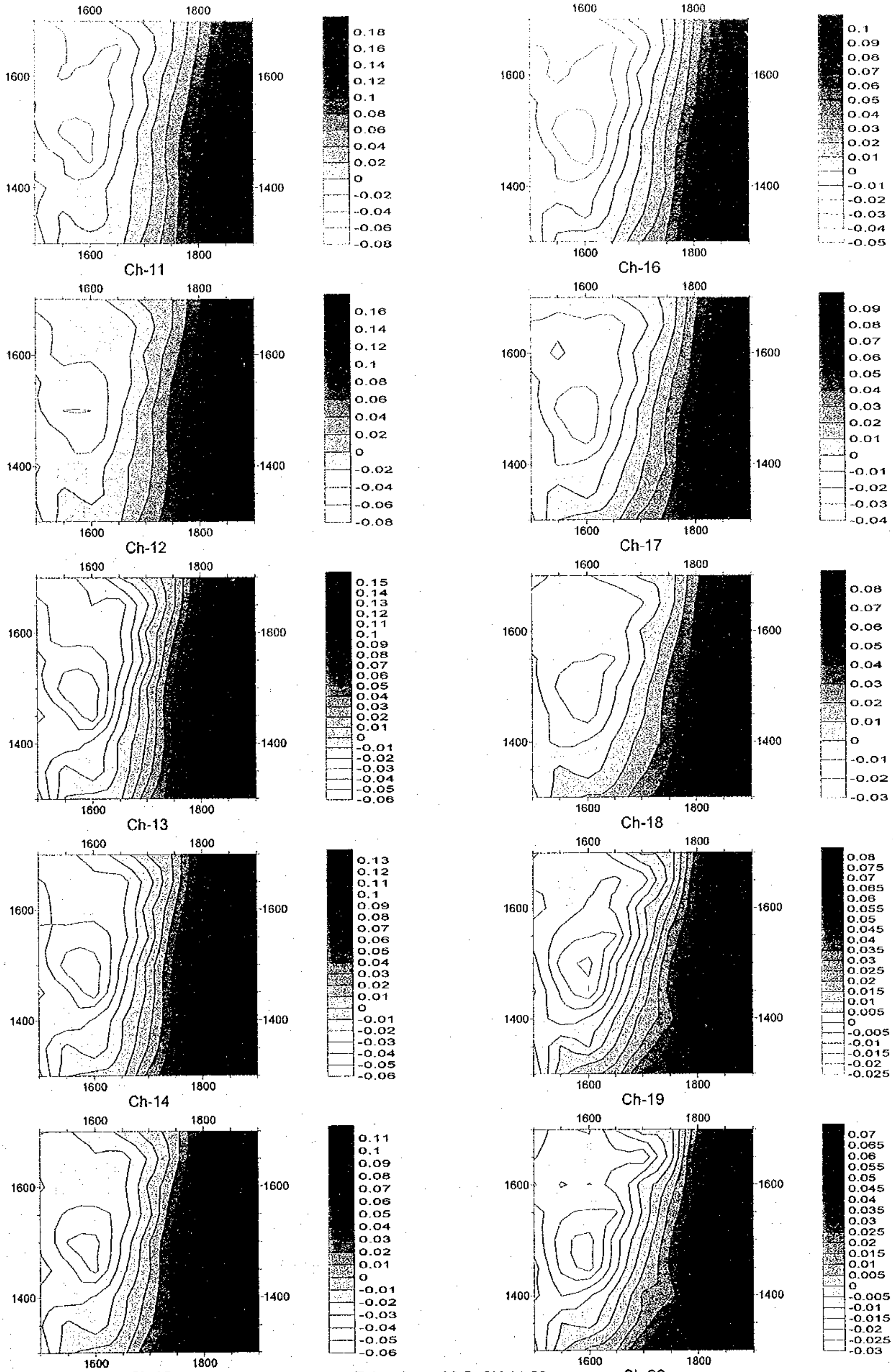


Fig. II-3-11(2) TEM response maps of Loop5 in Zuha area(Ch11-Ch20)

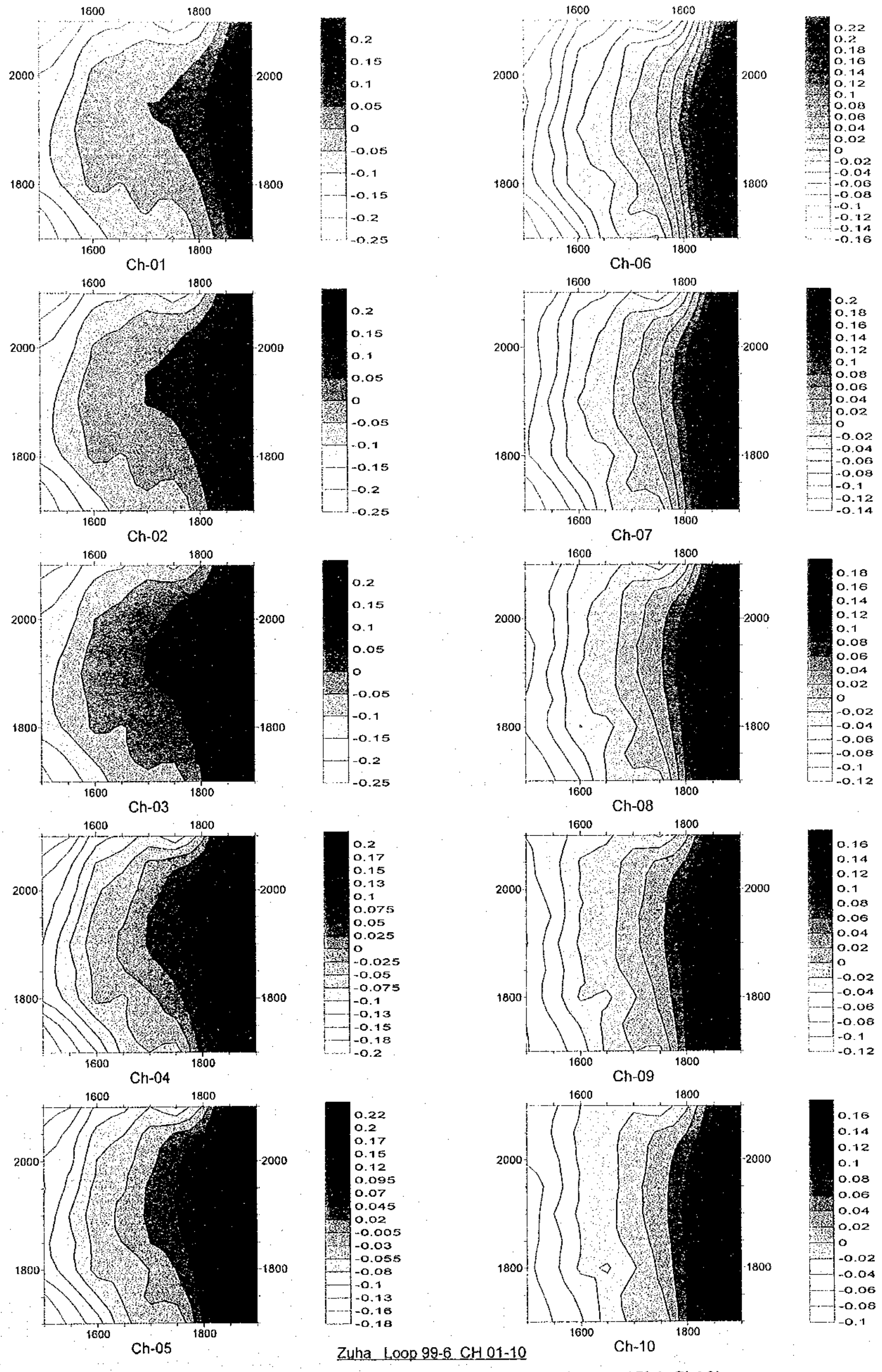


Fig. II-3-12(1) TEM response maps of Loop6 in Zuha area(Ch1-Ch10)

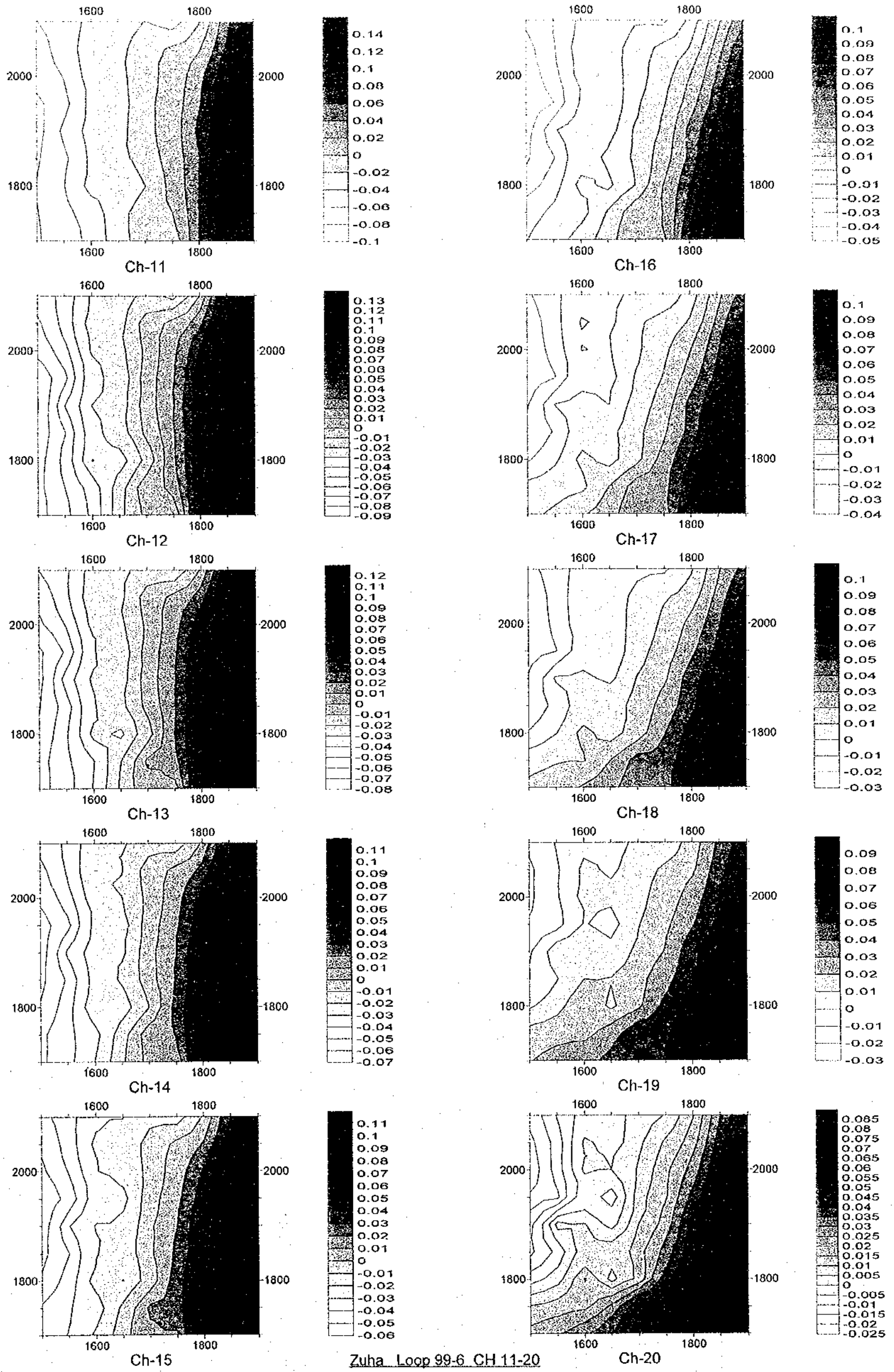


Fig. II-3-12(2) TEM response maps of Loop6 in Zuha area(Ch11-Ch20)

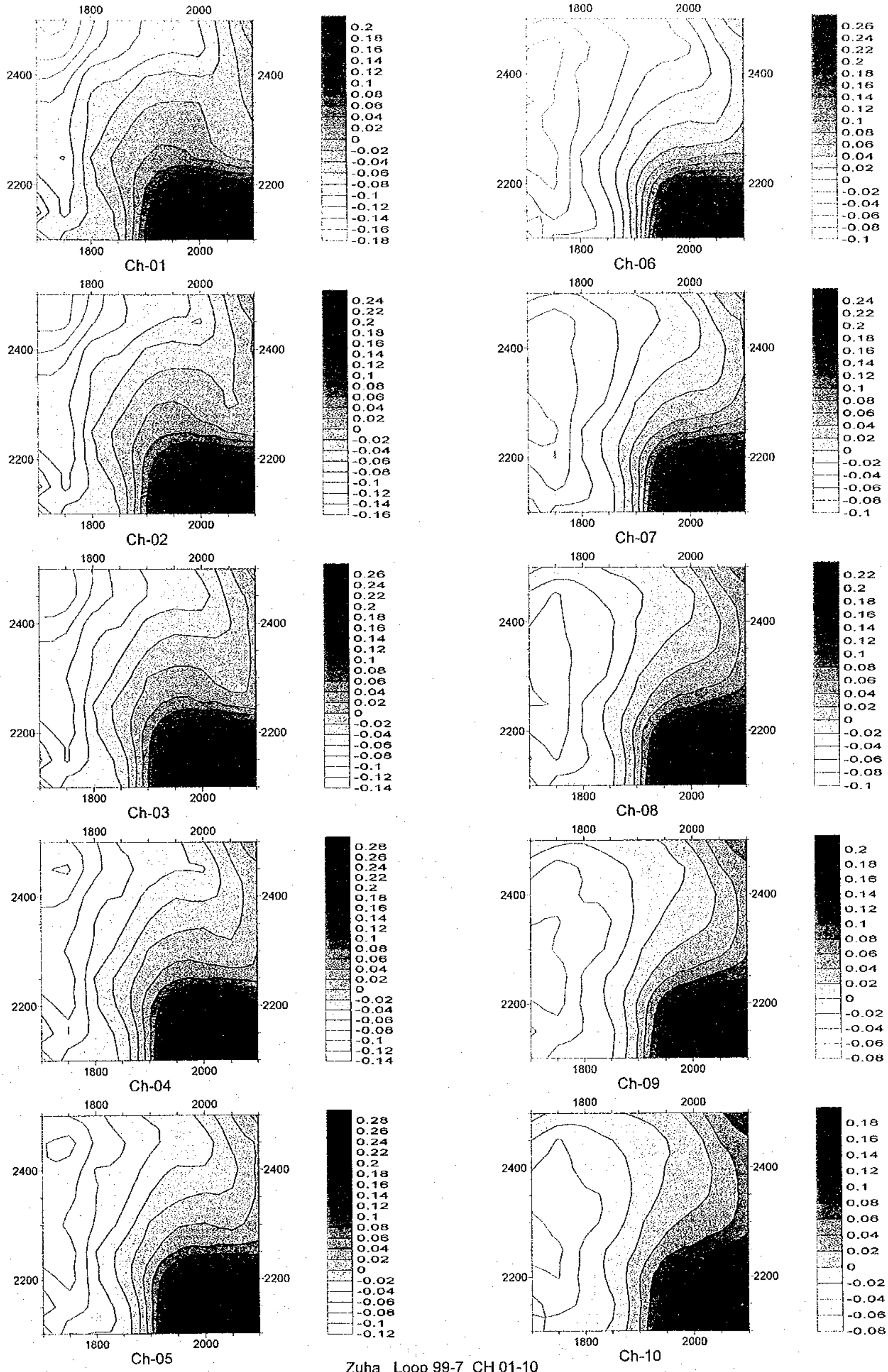


Fig. II-3-13(1) TEM response maps of Loop7 in Zuha area(Ch1-Ch10)

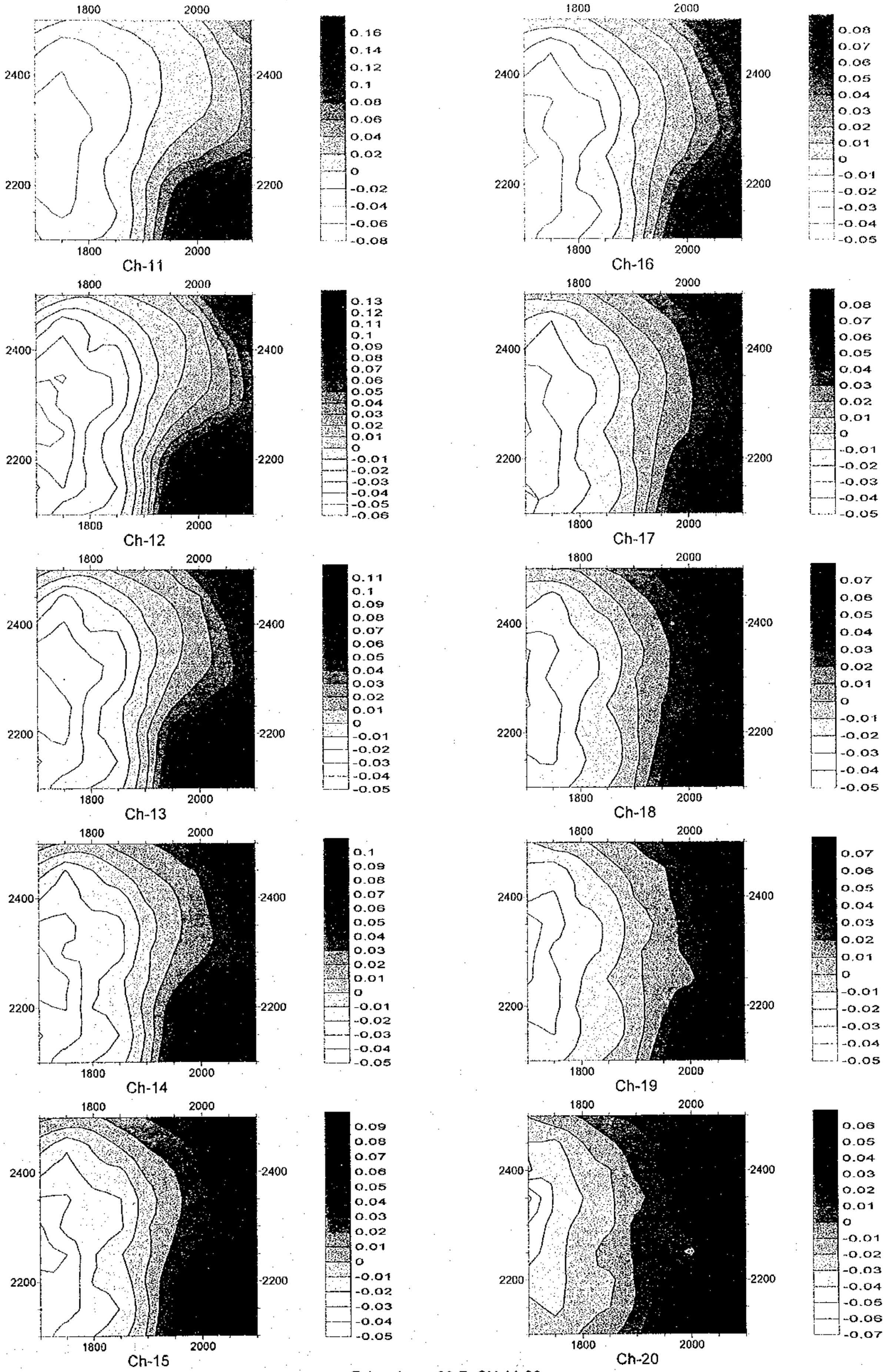


Zuha Loop 99-7 CH 11-20

Fig. II-3-13(2) TEM response maps of Loop7 in Zuha area(Ch11-Ch20)

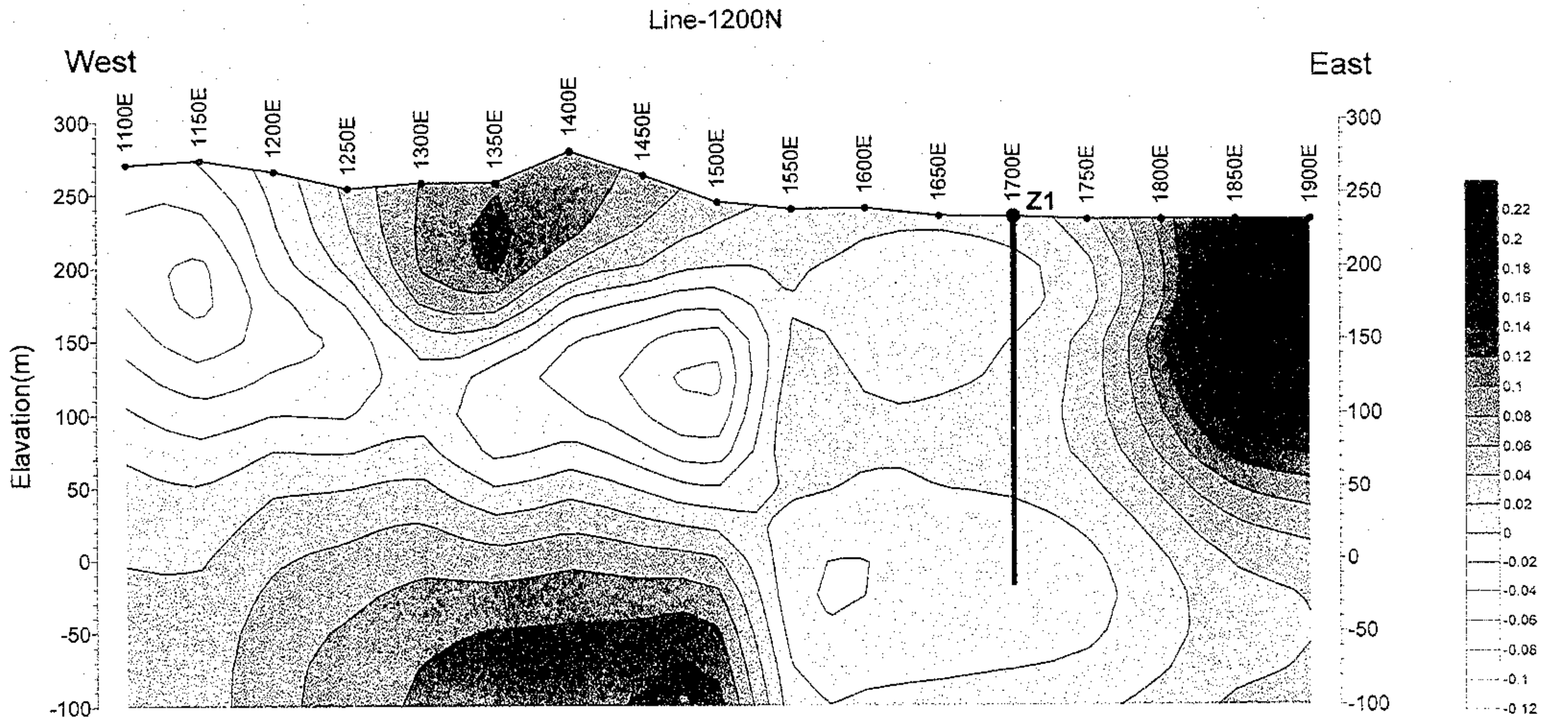


Fig. II-3-14 TEM response profile crossing drilling holes in Zuha area